

Changes in lumbar muscle diffusion tensor indices with age

| | |
|---------------|---|
| Item Type | Journal article |
| Authors | Weedall, Andrew;Dallaway, Alexander;Hattersley, John;Diokno, Michael;Hutchinson, Charles E.;Wilson, Adrian J.;Wayte, Sarah C. |
| Citation | Weedall, A.D., Dallaway, A., Hattersley, J. et al. (2024) Changes in lumbar muscle diffusion tensor indices with age. BJR Open, 6(1), tzae002,. |
| DOI | 10.1093/bjro/tzae002 |
| Publisher | Oxford University Press |
| Journal | BJR Open |
| Rights | Licence for published version: Creative Commons Attribution 4.0 International |
| Download date | 2026-06-18 13:41:06 |
| License | http://creativecommons.org/licenses/by/4.0/ |
| License | http://creativecommons.org/licenses/by/4.0/ |
| Link to Item | http://hdl.handle.net/2436/625525 |

Changes in lumbar muscle diffusion tensor indices with age

Andrew D. Weedall, MSc¹, Alexander Dallaway, PhD^{2,8}, John Hattersley, PhD^{3,4}, Michael Diokno, BSc⁵, Charles E. Hutchinson, MD^{5,6}, Adrian J. Wilson , PhD^{3,7,*}, Sarah C. Wayte, PhD¹

¹Radiology Physics, Department of Clinical Physics and Bioengineering, University Hospitals Coventry and Warwickshire NHS Trust, Coventry, CV2 2DX, United Kingdom

²Centre for Physical Activity, Sport and Exercise Sciences, Coventry University, Coventry, CV1 5FB, United Kingdom

³Human Metabolic Research Unit, Department of Research and Development, University Hospitals Coventry and Warwickshire NHS Trust, Coventry, CV2 2DX, United Kingdom

⁴School of Engineering, University of Warwick, Coventry, CV4 7AL, United Kingdom

⁵Radiology Department, University Hospitals Coventry and Warwickshire NHS Trust, Coventry, CV2 2DX, United Kingdom

⁶Warwick Medical School, University of Warwick, Coventry, CV4 7AL, United Kingdom

⁷Department of Physics, University of Warwick, Coventry, CV4 7AL, United Kingdom

⁸Present Address: Faculty of Education, Health and Wellbeing, School of Health and Society, University of Wolverhampton, Wolverhampton, WV1 1LY, United Kingdom

*Corresponding author: Adrian J. Wilson, PhD, Human Metabolic Research Unit, Department of Research and Development, University Hospitals Coventry and Warwickshire NHS Trust, Clifford Bridge Road, Coventry, CV2 2DX, United Kingdom (adrian.wilson@warwick.ac.uk; adrian.wilson3@nhs.net)

Abstract

Objective: To investigate differences in diffusion tensor imaging (DTI) parameters and proton density fat fraction (PDFF) in the spinal muscles of younger and older adult males.

Methods: Twelve younger (19-30 years) and 12 older (61-81 years) healthy, physically active male participants underwent T1_w, T2_w, Dixon and DTI of the lumbar spine. The eigenvalues (λ_1 , λ_2 , and λ_3), fractional anisotropy (FA), and mean diffusivity (MD) from the DTI together with the PDFF were determined in the multifidus, medial and lateral erector spinae (ESmed, ESlat), and quadratus lumborum (QL) muscles. A two-way ANOVA was used to investigate differences with age and muscle and *t*-tests for differences in individual muscles with age.

Results: The ANOVA gave significant differences with age for all DTI parameters and the PDFF ($P < .01$) and with muscle ($P < .01$) for all DTI parameters except for λ_1 and for the PDFF. The mean of the eigenvalues and MD were lower and the FA higher in the older age group with differences reaching statistical significance for all DTI measures for ESlat and QL ($P < .01$) but only in ESmed for λ_3 and MD ($P < .05$).

Conclusions: Differences in DTI parameters of muscle with age result from changes in both in the intra- and extra-cellular space and cannot be uniquely explained in terms of fibre length and diameter.

Advances in knowledge: Previous studies looking at age have used small groups with uneven age spacing. Our study uses two well defined and separated age groups.

Keywords: DTI; fat fraction; muscle; ageing.

Introduction

The age-related degeneration of muscle is characterized by a loss of muscle mass and strength.^{1,2} One impact of these changes, collectively termed sarcopenia,¹ is that it is associated with an increased risk of falls.^{1,3,4} The lumbar spinal muscles play an important role in rotation, flexion, extension, and stabilizing the spine^{5,6} and thus in maintaining balance. In sarcopenia, the loss of muscle mass is affected by factors other than age, including: the frequency and type of exercise;^{7,8} nutrition;^{9,10} and related co-morbidities (including diabetes mellitus, dementia, and cardiovascular disease¹¹). The loss of muscle strength in sarcopenia is much greater than predicted by loss of muscle mass¹ suggesting there may also be changes in the number, type, diameter, and organization of fibres within the muscle.¹²⁻¹⁵ The impact muscle ageing has on the quality of life for individuals in an ageing population means non-invasive methods are required to investigate the changes in muscle with age.

An increase in the fat content of muscle is a key component of the definition of muscle ageing^{1,2} and MRI determined proton density fat fraction (PDFF) is a quantitative measure of tissue adiposity. This measure, calculated from data acquired using chemical shift encoded water-fat MRI (Dixon imaging), indicates the global adiposity in an area of interest. Previous work has shown that muscle adiposity inversely correlates with strength^{16,17} and that this measure is a better predictor of muscle strength than cross-sectional area.¹⁸ Changes in muscle with age occur in conjunction with an increase in the mass of fat^{12,16} and connective tissue¹⁹ in the extra-cellular space, which contributes to a change in body composition. Whilst quantifying changes in the fat content of muscle is important in describing changes in muscle with age, it gives no information about changes in the muscle fibres or their organization.

Diffusion tensor imaging (DTI) is a quantitative method of assessing the movement of water molecules in tissue due to

Received: 20 November 2023; Accepted: 10 January 2024

© The Author(s) 2024. Published by Oxford University Press on behalf of the British Institute of Radiology.

This is an Open Access article distributed under the terms of the Creative Commons Attribution License (<https://creativecommons.org/licenses/by/4.0/>), which permits unrestricted reuse, distribution, and reproduction in any medium, provided the original work is properly cited.

Brownian motion.²⁰ The parameters used to quantify DTI are the eigenvalues (λ_1 , λ_2 , and λ_3), from which two further parameters, fractional anisotropy (FA) and mean diffusivity (MD), are derived. The numerical values of these are determined by tissue microstructure constraining movement of water molecules. Age-related degeneration of muscle tissue has been shown to include changes in the structure of skeletal muscle,^{15,21,22} including fibre types and diameters.¹² Previous work on the large muscles of the legs have attributed changes in numerical parameters from DTI to changes in muscle fibre type, size, and orientation.^{14,23-25} DTI has also been used to investigate how the tissue microstructure responds to exercise²⁶ and injury.²⁷ DTI parameters in the spinal musculature have been shown to be consistent with those from other muscles, poorly correlated with body mass index (BMI)⁶ and to predict muscle strength.¹⁶ Changes in the DTI parameters of the spinal musculature have also been shown to be associated with lumbar spinal disease.⁵

The study reported in this article aimed to investigate whether there were differences in the PDFF and DTI parameters of the spinal muscles between younger and older physically active adult males. Our hypothesis was that differences in the DTI parameters in the older group when compared to the younger group of participants would give evidence for DTI providing a non-invasive probe of changes in tissue microstructure reported in histological studies.¹²

Materials and methods

This study was part of a wider investigation into muscle ageing in healthy male participants,²⁸ which had ethical approval from the Coventry University Ethics Committee (reference P70399). The study was carried out in compliance with the Ethical Principles for Medical Research on Human Subjects set down in the Declaration of Helsinki by the World Medical Association. All participants provided written informed consent for the MRI data acquisition.

Participants

Two groups of healthy, physically active adult male participants, one younger ($n=12$) and one older ($n=12$) were recruited as described by Dallaway et al.²⁸ Inclusion criteria for this study were: healthy males aged 18-30 years; and healthy males aged 60 years or older. Exclusion criteria were: BMI outside of the range 18.5-29.9 kg.m⁻²; smokers; daily alcohol consumption; and an existing or past history of metabolic disease, neuromuscular disorders or musculoskeletal impairments that affect muscular strength. Table 1 shows the demographic data for the two groups.

Data acquisition

Participants were scanned head-first, supine, on a GE Discovery 750 w 3 T scanner (GE Healthcare, Amersham, UK) using the 40-element spine array coil built into the scanning couch. Axial images were obtained from approximately the third lumbar vertebra to the fifth lumbar vertebra allowing visualization of the lumbar spinal muscles (quadratus lumborum [QL], erector spinae [lateral—ESlat and medial—ESmed] and multifidus [MF]) at these levels. T1_w imaging, T2_w imaging, Dixon imaging, and DTI were performed on each participant. Fat-only and water-only images were obtained of the lumbar spinal muscles using a 3D gradient echo IDEAL IQ sequence.²⁹ The parameters used are shown in Table 2.

Table 1. Participant demographic data giving the mean \pm SD (range).

| | Age group | |
|------------------------|-----------------------------|-----------------------------|
| | Younger | Older |
| Age/years | 24.7 \pm 3.1 (19-30) | 67.3 \pm 6.0 (61-81) |
| Height/m | 1.78 \pm 0.1 (1.65-1.89) | 1.74 \pm 0.1 (1.63-1.87) |
| Weight/kg | 76.4 \pm 11.2 (57.4-91.9) | 79.2 \pm 10.8 (56.0-93.5) |
| BMI/kg m ⁻² | 24.1 \pm 2.2 (21.1-27.1) | 26.0 \pm 2.7 (21.1-29.9) |

Table 2. IDEAL IQ imaging parameters.

| Parameter | Value |
|--------------------|--------------------|
| TR/TE | 16.6/5.1 ms |
| Receiver bandwidth | 111 kHz |
| FoV | 24 cm ² |
| Slice thickness | 4 mm |
| Matrix | 224 \times 224 |
| Flip angle | 6° |
| Number of averages | 4 |
| Acquisition time | 8 min 12 s |

Table 3. DTI imaging parameters.

| Parameter | Value |
|----------------------|---------------------------|
| TR/TE | 800/63 ms |
| Receiver bandwidth | 250 kHz |
| FoV | 24 cm ² |
| Slice thickness | 4 mm |
| Matrix | 96 \times 96 |
| Diffusion directions | 15 |
| <i>b</i> -values | 0, 450 s.mm ⁻² |
| Number of averages | 4 |
| Acquisition time | 8 min 40 s |

The DTI was performed using a single-shot echo planar imaging technique with spectral fat saturation using the parameters shown in Table 3.

The image sets were acquired sequentially without repositioning the subject with all scans performed between the same axial start and end points, with the same field of view and with the same slice thickness. In addition, a scanner utility “copy coverage” was used to ensure all images had the same inferior-superior coverage. Each slice in the 30 image sets were interpolated to 256 \times 256 pixels before being stored in DICOM format. All image processing was done on these DICOM images.

Data analysis

For each participant in the study, the slice including the superior end plate of the third lumbar vertebra (denoted L3ep) and the slice including the superior end plate of the fourth lumbar vertebra (denoted L4ep) were identified manually (by A.J.W. and A.D.W.) from the T1_w and T2_w images using ImageJ (<https://imagej.nih.gov/>). All images were then converted from DICOM to NIfTI format using the Matlab routine dicm2nii (<https://github.com/xiangruili/dicm2nii>). Using FSLeyes (<https://fsl.fmrib.ox.ac.uk/fsl/fslwiki/FSLeyes>), circular regions of interest (ROIs) were drawn on slices in the T1_w image slices at L3ep and L4ep on the left and right side of the body in the muscle being studied. Binary masks were then created for these ROIs (Figure 1). For each participant the diameter of the ROIs was the same for all four sites of the same

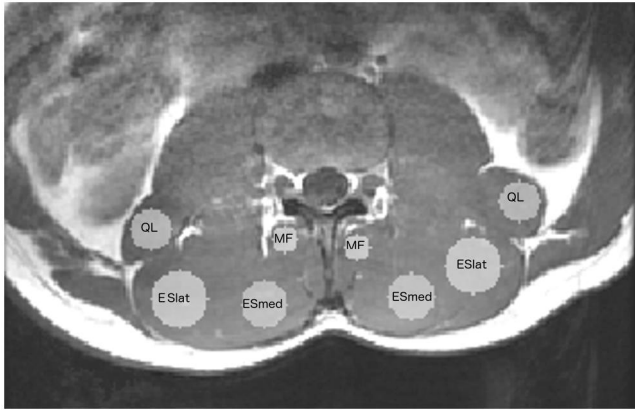


Figure 1. An example of the circular regions of interest (ROIs) in the muscles studied on the L3ep slice of a T_{1w} image. The diameter of the ROI for each muscle was the largest that could be fitted into all four sites (right and left for L3ep and L4ep) excluding regions of fat for that muscle.

muscle and was the largest possible ROI contained wholly in the muscle avoiding obvious regions of fat.

Proton density fat fraction

The PDFF data were determined using a method based on previous work³⁰ in the ROIs created for each muscle site. If f_i and w_i are pixels from the fat only and water-only images, respectively, in an ROI then the fat fraction (PDFF) for that pixel, ff_i is given by:

$$ff_i = \frac{f_i}{f_i + w_i}, \quad (1)$$

and the average PDFF for the ROI, PDFF_{roi}, is given by:

$$\text{PDFF}_{\text{roi}} = \frac{\sum_{i=1}^{N_i} ff_i}{N_i}. \quad (2)$$

The PDFF for each muscle studied is taken as the average value of PDFF_{roi} for all ROIs in that muscle.

Diffusion tensor imaging

The eigenvalues of the diffusion tensors were determined within the circular ROIs using the tensor fitting model within DIPY (<https://dipy.org>) from which the FA and MD were calculated. The mean values for these parameters were then calculated for each ROI. From these, average values for the eigenvalues, FA, and MD were then calculated for each muscle for each participant.

Statistical analysis

Statistical comparisons of λ_1 , λ_2 , λ_3 , FA, MD, and PDFF between age groups and muscles were performed in R (<https://www.r-project.org>) using a two-way ANOVA. Where there was a statistically significant difference between muscles a Tukey HSD follow-up analysis was performed between pairs of muscle sites. In addition, differences with age were further investigated to determine whether these were muscle dependant using *t*-tests to compare the age groups for each muscle independently. Statistical significance was taken as $P < .05$ throughout. Corrected probability values are reported for the Tukey

Table 4. The mean \pm SD for the diameters of the ROIs in pixels (0.96 mm) for the different muscles.

| Muscle | Younger | Older |
|--------------------------------|------------------|------------------|
| Multifidus (MF) | 3.33 \pm 0.65 | 1.92 \pm 0.79 |
| Erectus spinae—lateral (ESlat) | 11.25 \pm 1.22 | 7.67 \pm 1.87 |
| Erectus spinae—medial (ESmed) | 9.50 \pm 1.83 | 7.58 \pm 1.24 |
| Quadratus lumborum (QL) | 14.25 \pm 0.87 | 12.50 \pm 1.73 |

Abbreviations: SD = standard deviation; ROI=region of interest.

HSD analysis and a Bonferroni correction for multiple comparisons was applied to probability values from the *t*-test analyses.

Results

For the ESlat, ESmed, and MF muscles, ROIs could be created for all four sites, however, for the QL muscle it was not possible to create ROIs at the L4ep level in all participants. In four participants from the younger group and all participants in the older age group, the L4ep was below the superior surface of the iliac fossa and hence below the inferior extent of the QL muscle. Thus, no measurement for the QL muscle at the L4ep level could not be made and DTI parameters for the QL are only from the L3ep level.

The diameter of the ROIs was consistently higher in the younger group than the older group (Table 4), primarily due to a greater volume of fat within the muscle of the older group. With the exception of the ROI for ESmed, the variation in the diameter of the ROIs between subjects was greater in the older group than in the younger group.

Figure 2 shows the individual PDFF values for each of the muscles studied together with the mean and SD from Table 5.

The two-way ANOVA on these data showed a statistically significant difference in PDFF with both age ($P < .01$) and muscle ($P < .01$), with a significant interaction between age and muscle ($P < .05$). The only significant differences between pairs of muscles in the follow-up analysis to the ANOVA were between ESmed and MF ($P < .01$), ESlat and MF ($P < .01$), QL and MF ($P < .01$), and between ESmed and QL ($P < .05$) (Table 6).

From Figure 2, it can be seen that the mean PDFF was higher in the older group with *t*-tests giving statistically significant differences for MF, ESlat, and QL at $P < .01$ but not for ESmed ($P > .05$).

Figure 3 shows individual values for each of the DTI parameters with the mean \pm SD values from Table 7 superimposed on them.

The results of the 2-way ANOVA on these data gave a statistically significant difference for all the DTI parameters with both age ($P < .01$) and between muscles ($P < .01$) for all measures except λ_1 . There was no interaction between age and muscle for any of the DTI parameters ($P > .05$).

The results for the post-ANOVA analysis of differences in the DTI parameters between pairs of muscles are summarized in Table 8. It is interesting to note that the number of significant differences between muscles is much larger for λ_3 than for the other eigenvalues.

The *t*-tests between pairs of muscles (Figure 3) showed statistically significantly lower values for all three eigenvalues in the older group for ESlat and QL (all $P < .01$). ESmed only gave a significant difference for λ_3 ($P < .05$). There were statistically significantly higher values of FA in the older group for ESlat and QL (both $P < .01$) but not for ESmed ($P > .05$) and statistically

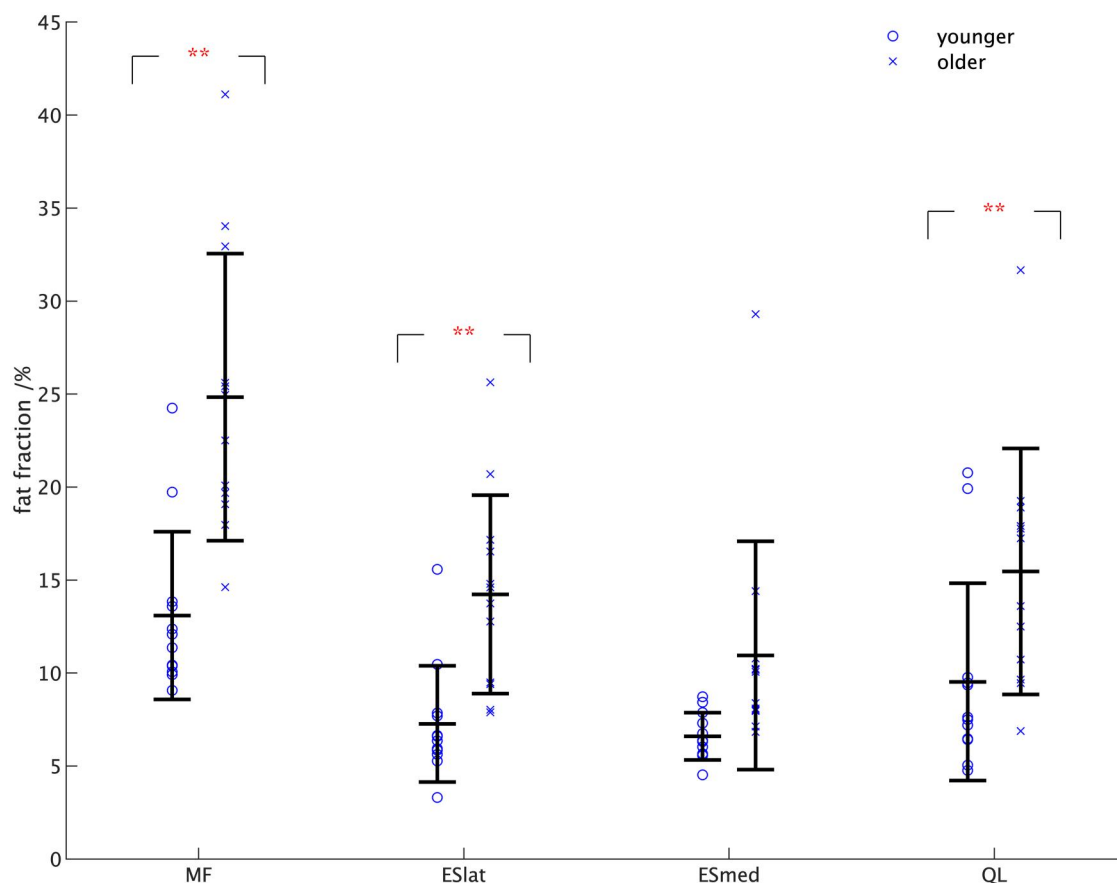


Figure 2. The individual values for the PDFF within the ROIs. The values of the mean \pm standard deviation for each muscle (Table 5) are shown together with the results of the t-test comparisons between muscles ($*P < .05$, $**P < .01$). Abbreviations: PDFF = proton density fat fraction; ROIs = regions of interest.

Table 5. The mean \pm SD of the PDFF for each muscle expressed as a % in each age group.

| | MF | ESlat | ESmed | QL |
|---------|------------------|------------------|-----------------|------------------|
| Younger | 13.09 \pm 4.51 | 7.27 \pm 3.13 | 7.23 \pm 1.36 | 9.52 \pm 5.31 |
| Older | 24.83 \pm 7.72 | 14.23 \pm 5.34 | 9.69 \pm 2.09 | 15.46 \pm 6.61 |

Abbreviations: SD = standard deviation; PDFF = proton density fat fraction.

Table 6. Post-ANOVA analysis of differences in PDFF between pairs of muscles ($-P > .05$, $*P < .05$, $**P < .01$).

| Muscle 1 | Muscle 2 | P |
|----------|----------|----|
| MF | ESlat | ** |
| MF | ESmed | ** |
| MF | QL | ** |
| ESlat | ESmed | - |
| ESlat | QL | - |
| ESmed | QL | * |

Abbreviations: ANOVA = analysis of variance; PDFF = proton density fat fraction.

significantly lower values of MD in the older age group for ESlat and QL ($P < .01$), ESmed ($P < .05$) but not for MF.

Discussion

As expected, the results show an increase in PDFF in the older group in all muscles, consistent with descriptions of muscle

ageing¹⁻³ and with studies finding a negative correlation between muscle mass and age,²² including in the muscles, we studied.³¹ Whilst the PDFF was higher in the older group for all muscles studied, it was not statistically significant in all muscles. This together with the significant interaction between age and muscle from the ANOVA analysis suggests that changes in PDFF in the spinal musculature with age are muscle dependant.

For the DTI parameters, our results showed lower values for all of the eigenvalues and MD in the older group for all muscles studied, with the differences being statistically significant for all these measures in ESlat and QL but only for λ_3 and MD in ESmed. The difference for MF did not reach statistical significance for any of these measures. The FA was shown to be higher in the older group for all muscles studied, again with the differences being statistically significant in all the muscles studied except for ESmed and MF. Our results for the eigenvalues were consistent with the findings of one previous study,¹⁴ but not another where increases in all eigenvalues with age were reported.¹³ Consistent with our findings, not all differences with age reached statistical significance in all muscles included in these studies.^{13,14} Another study only reporting FA and MD found no significant change in FA with age³² inconsistent with our findings and one other study,¹³ but not with the findings from another study.¹⁴ However, the value of MD from the same study³² showed a significant increase with age, which is inconsistent with our findings. Loss of muscle strength is associated with muscle ageing^{1,12} and a positive correlation has

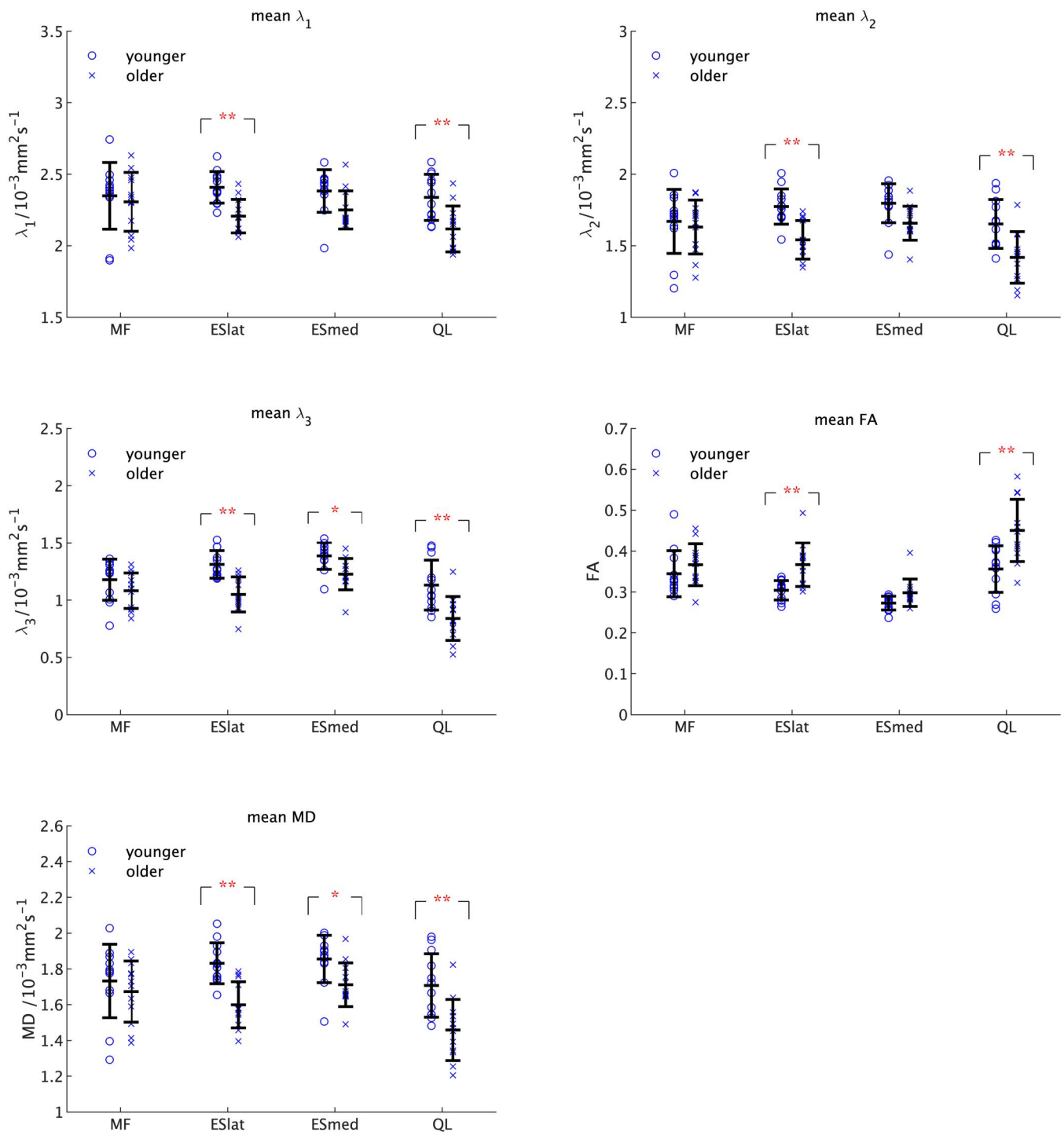


Figure 3. The individual values of the DTI parameters for each muscle. These are shown together with the mean and standard deviations for each muscle in each age group (Table 7). Results of the *t*-test analysis of differences between age groups for each muscle are shown (* $P < .05$, ** $P < .01$). Abbreviation: DTI = diffusion tensor imaging.

been reported between the eigenvalues, MD and radial diffusivity ($\text{RD} = [\lambda_2 + \lambda_3]/2$), and strength in the spinal musculature.¹⁶ Therefore, a decrease in the eigenvalues with age would be expected, consistent with our results. Theoretical work concluded that increasing fibre diameter is the largest determinant of increasing values of λ_2 and λ_3 ,²⁵ a conclusion supported by a negative correlation between the proportion of type I fibres and RD reported in an experimental study³³ as type II fibres have a larger diameter than type I fibres. This together with histology

studies showing a preferential reduction in the diameter of type II fibres with age^{12,34} further supports our finding of reduced values of λ_2 and λ_3 in the older group. The lack of consistency in findings with age between studies and even between muscles within the same subject^{13,14} needs an explanation. Whilst understanding the results obtained for PDFF in terms of the expected changes with ageing is straightforward, the same is not true for the DTI parameters. Although the number of studies comparing DTI parameters with age is small, there is a

Table 7. The mean \pm SD of the DTI parameters for the younger and older age groups.

| Muscle position | Age group | DTI parameter | | | | |
|--------------------------------|-----------|--|--|--|-----------------|---|
| | | λ_1 / 10^{-3} mm ² s ⁻¹ | λ_2 / 10^{-3} mm ² s ⁻¹ | λ_3 / 10^{-3} mm ² s ⁻¹ | FA | MD / 10^{-3} mm ² s ⁻¹ |
| Multifidus (MF) | Younger | 2.35 \pm 0.23 | 1.67 \pm 0.22 | 1.18 \pm 0.18 | 0.34 \pm 0.06 | 1.73 \pm 0.21 |
| | Older | 2.31 \pm 0.21 | 1.63 \pm 0.19 | 1.08 \pm 0.15 | 0.37 \pm 0.05 | 1.67 \pm 0.17 |
| Erectus spinae—lateral (ESlat) | Younger | 2.41 \pm 0.11 | 1.77 \pm 0.12 | 1.31 \pm 0.12 | 0.30 \pm 0.02 | 1.83 \pm 0.11 |
| | Older | 2.21 \pm 0.12 | 1.54 \pm 0.13 | 1.05 \pm 0.15 | 0.37 \pm 0.05 | 1.60 \pm 0.13 |
| Erectus spinae—medial (ESmed) | Younger | 2.38 \pm 0.15 | 1.80 \pm 0.14 | 1.39 \pm 0.12 | 0.27 \pm 0.02 | 1.86 \pm 0.13 |
| | Older | 2.25 \pm 0.13 | 1.66 \pm 0.12 | 1.23 \pm 0.14 | 0.30 \pm 0.03 | 1.71 \pm 0.12 |
| Quadratus lumborum (QL) | Younger | 2.34 \pm 0.16 | 1.65 \pm 0.17 | 1.13 \pm 0.22 | 0.36 \pm 0.06 | 1.71 \pm 0.18 |
| | Older | 2.12 \pm 0.16 | 1.42 \pm 0.18 | 0.84 \pm 0.19 | 0.45 \pm 0.08 | 1.46 \pm 0.17 |

Abbreviations: SD = standard deviation; DTI = diffusion tensor imaging.

Table 8. Post-ANOVA analysis of differences between pairs of muscles ($P > .05$, * $P < .05$, ** $P < .01$).

| Muscle 1 | Muscle 2 | DTI parameter | | | | |
|----------|----------|---------------|-------------|-------------|----|----|
| | | λ_1 | λ_2 | λ_3 | FA | MD |
| MF | ESlat | – | – | – | – | – |
| MF | ESmed | – | – | ** | ** | – |
| MF | QL | – | – | ** | ** | ** |
| ESlat | ESmed | – | – | ** | ** | – |
| ESlat | QL | – | – | ** | ** | ** |
| ESmed | QL | – | * | ** | ** | ** |

Abbreviation: ANOVA = analysis of variance.

larger body of literature on theoretical models,²⁵ and studies aimed at correlating DTI measures with muscle strength¹⁶ that contribute to the interpretation.

Ageing reduces the number of fibres¹⁵ and shows selective atrophy of the larger diameter, type II, fibres,^{35–37} reducing the average diameter of the fibres, increases the volume of the extra-cellular space, which must have an impact on the eigenvalues. Sinha et al,¹³ based on the work of Galban et al³⁸ and Krampinos et al,³⁹ proposed a weighted sum model based on “fibre fraction” to describe how the fibres and extra-cellular space contribute to a final value for λ_1 , λ_2 , and λ_3 . This model is based on the view that the eigenvalues calculated from images are the result of the properties of the fibres and the extra-cellular compartment. An assumption implicit in the weighted sum model¹³ is that molecular movement in the extra-cellular space is isotropic, which leads to the logical conclusion that λ_1 should remain unchanged or increase with ageing as the fat content of muscle increases.¹ However, the extra-cellular space is not homogeneous but contains fat cells, connective tissue, and necrotized fibres—a content that will increase with age^{12,40} giving barriers that restrict movement of water molecules hence reducing all 3 eigenvalues. Thus, this linear representation of the fibres and extra-cellular space using a single value, the (cross-sectional) fibre fraction, to describe the properties of both the fibres and the extra-cellular space appears to be an over-simplification. However, this model does establish the important principle that changes in the value of each eigenvalue with age (and consequently FA and MD) are the result of changes in both the fibres and the extra-cellular space.

Conclusion

We have shown an increase in PDFF and a decrease in eigenvalues in the lumbar muscles of older individuals. The

components of muscle ageing, which include changes in both the fibres and the extra-cellular space occur at different rates in different individuals over a long period of time. Therefore, it is perhaps an over-simplification to explain the changes in eigenvalues in terms of fibre diameter and length. Moreover, current knowledge means it is impossible to uniquely relate changes in eigenvalues to changes in fibres and the extra-cellular space.

Acknowledgements

We would like to thank GE for their on-going support in maintaining the research agreement with UHCW. We also thank the MRI radiographers at UHCW, Research Nurse Alison Campbell, and her nursing team for collection of the BMI data and David Dixon for technical support with this.

Funding

None declared.

Conflicts of interest

None declared.

Data availability

The data underlying this article will be shared on reasonable request to Sonia Kandola, Research Governance and Quality Manager, Research and Development Department, University Hospitals Coventry and Warwickshire NHS Trust, Coventry, CV2 2DX, UK.

References

- Boutin RD, Yao L, Canter RJ, Lenchik L. Sarcopenia: current concepts and imaging implications. *AJR Am J Roentgenol.* 2015;205(3):W255–W266.
- Rosenberg IH. Sarcopenia: origins and clinical relevance. *J Nutr.* 1997;127(5 Suppl):990S–991S.
- Janssen I, Heymsfield S, Ross R. Low relative skeletal muscle mass (sarcopenia) in older persons is associated with functional impairment and physical disability. *J Am Geriatr Soc.* 2002;50(5):889–896.
- Hong W, Cheng Q, Zhu X, et al. Prevalence of sarcopenia and its relationship with sites of fragility fractures in elderly Chinese men and women. *PLoS One.* 2015;10(9):e0138102.

5. Oh J, Jung J, Ko Y. Can diffusion tensor imaging and tractography represent cross-sectional area of lumbar multifidus in patients with lumbar spine disease? *Muscle Nerve*. 2018;57(2):200-205.
6. Jones G, Kumbhare D, Harish S, Noseworthy M. Quantitative DTI assessment in human lumbar stabilization muscles at 3 T. *J Comput Assist Tomogr*. 2013;37(1):98-104.
7. Nascimento C, Ingles M, Salvador-Pascual A, Cominetti M, Gomez-Cabrera M, Viña J. Sarcopenia, frailty and their prevention by exercise. *Free Radic Biol Med*. 2019;132:42-49.
8. Phu S, Boersma D, Duque G. Exercise and sarcopenia. *J Clin Densitom*. 2015;18(4):488-492.
9. Naseeb M, Volpe S. Protein and exercise in the prevention of sarcopenia and aging. *Nutr Res*. 2017;40:1-20.
10. Anton SD, Hida A, Mankowski R, et al. Nutrition and exercise in sarcopenia. *Curr Protein Pept Sci*. 2018;19(7):649-667.
11. Pacifico J, Geerlings MAJ, Reijnierse EM, Phassouliotis C, Lim WK, Maier AB. Prevalence of sarcopenia as a comorbid disease: a systematic review and meta-analysis. *Exp Gerontol*. 2020;131:110801.
12. Doherty TJ. Physiology of ageing. *J Appl Physiol (1985)*. 2003;95(4):1717-1727.
13. Sinha U, Csapo R, Malis V, Xue Y, Sinha S. Age-related differences in diffusion tensor indices and fibre architecture in the medial and lateral gastrocnemius. *J Magn Reson Imaging*. 2015;41(4):941-953.
14. Galban CJ, Maderwald S, Stock F, Ladd ME. Age-related changes in skeletal muscle as detected by diffusion tensor magnetic resonance imaging. *J Gerontol A Biol Sci Med Sci*. 2007;62(4):453-458.
15. Narici MV, Maffulli N. Sarcopenia: characteristics, mechanisms and functional significance. *Br Med Bull*. 2010;95:139-159.
16. Klupp E, Cervantes B, Schlaeger S, et al. Paraspinal muscle DTI metrics predict muscle strength. *J Magn Reson Imaging*. 2019;50(3):816-823.
17. Baum T, Inhuber S, Dieckmeyer M, et al. Association of quadriceps muscle fat with isometric strength measurements in healthy males using chemical shift encoding-based water-fat magnetic resonance imaging. *J Comput Assist Tomogr*. 2016;40(3):447-451.
18. Schlaeger S, Inhuber S, Rohrmeier A, et al. Association of paraspinal muscle water-fat MRI-based measurements with isometric strength measurements. *Eur Radiol*. 2019;29(2):599-608.
19. Khalil C, Hancart C, Le Thuc V, Chantelot C, Chechin D, Cotten A. Diffusion tensor imaging and tractography of the median nerve in carpal tunnel syndrome: preliminary results. *Eur Radiol*. 2008;18(10):2283-2291.
20. Minati L, Węglarz WP. Physical foundations, models, and methods of diffusion magnetic resonance imaging of the brain: a review. *Concepts Magn Reson*. 2007;30A(5):278-307.
21. Goldspink G. Age-related muscle loss and progressive dysfunction in mechanosensitive growth factor signaling. *Ann N Y Acad Sci*. 2004;1019:294-298.
22. Janssen I, Heymsfield SB, Wang ZM, Ross R. Skeletal muscle mass and distribution in 468 men and women aged 18–88 yr. *J Appl Physiol (1985)*. 2000;89(1):81-88.
23. Li K, Dortch RD, Welch EB, et al. Multi-parametric MRI characterization of healthy human thigh muscles at 3.0 T—relaxation, magnetization transfer, fat/water, and diffusion tensor imaging. *NMR Biomed*. 2014;27(9):1070-1084.
24. Budzik J, Balbi V, Verclytte S, Pansini V, Thuc V, Cotten A. Diffusion tensor imaging in musculoskeletal disorders. *Radiographics*. 2014;34(3):E56-E72.
25. Berry D, Regner B, Galinsky V, Ward S, Frank L. Relationships between tissue microstructure and the diffusion tensor in simulated skeletal muscle. *Magn Reson Med*. 2017;80(1):317-329.
26. Yanagisawa O, Kurihara T, Kobayashi N, Fukubayashi T. Strenuous resistance exercise effects on magnetic resonance diffusion parameters and muscle-tendon function in human skeletal muscle. *J Magn Reson Imaging*. 2011;34(4):887-894.
27. McMillan AB, Shi D, Pratt SJ, Lovering RM. Diffusion tensor MRI to assess damage in healthy and dystrophic skeletal muscle after lengthening contractions. *J Biomed Biotechnol*. 2011;2011:970726.
28. Dallaway A, Hattersley J, Diokno M, et al. Age-related degeneration of lumbar muscle morphology in healthy younger versus older men. *Aging Male*. 2020;23(5):1583-1597.
29. Reeder S, Pineda A, Wen Z, et al. Iterative decomposition of water and fat with echo asymmetry and least-squares estimation (IDEAL): application with fast spin-echo imaging. *Magn Reson Med*. 2005;54(3):636-644.
30. Weedall AD, Wilson AJ, Wayte SC. An investigation into the effect of body mass index on the agreement between whole-body fat mass determined by MRI and air-displacement plethysmography. *Br J Radiol*. 2019;92(1103):20190300.
31. Crawford RJ, Volken T, Mhuiris AN, et al. Geography of lumbar paravertebral muscle fatty infiltration. *Spine (Phila Pa 1976)*. 2019;44(18):1294-1302.
32. Farrow M, Biglands J, Tanner SF, et al. The effect of ageing on skeletal muscle as assessed by quantitative MR imaging: an association with frailty and muscle strength. *Aging Clin Exp Res*. 2021;33(2):291-301.
33. Scheel M, von Roth P, Winkler T, et al. Fibre type characterisation in skeletal muscle by diffusion tensor imaging. *NMR Biomed*. 2013;26(10):1220-1224.
34. Alnaqeb MA, Al Zaid NS, Goldspink G. Connective tissue changes and physical properties of developing and ageing skeletal muscle. *J Anat*. 1984;139(Pt 4):677-689.
35. Evans W, Lexell J. Human aging, muscle mass, and fiber type composition. *J Gerontol A Biol Sci Med Sci*. 1995;50:11-16.
36. Andersen J. Muscle fibre type adaptation in the elderly human muscle. *Scand J Med Sci Sports*. 2003;13(1):40-47.
37. Nilwik R, Snijders T, Leenders M, et al. The decline in skeletal muscle mass with aging is mainly attributed to a reduction in type II muscle fiber size. *Exp Gerontol*. 2013;48(5):492-498.
38. Galban CJ, Maderwald S, Uffmann K, de Greiff A, Ladd ME. Diffusive sensitivity to muscle architecture: a magnetic resonance diffusion tensor imaging study of the human calf. *Eur J Appl Physiol*. 2004;93(3):253-262.
39. Karampinos DC, King KF, Sutton BP, Georgiadis JG. Myofibre ellipticity as an explanation for transverse asymmetry of skeletal muscle diffusion MRI in vivo signal. *Ann Biomed Eng*. 2009;37(12):2532-2546.
40. Doherty TJ. Aging and sarcopenia. *J Appl Physiol (1985)*. 2003;95(4):1717-1727.